

New Aspects Providing Transformer Models

Marius-Constantin O.S. Popescu, Nikos E. Mastorakis, Liliana N. Popescu-Perescu

Abstract—In this paper, on basis of heat transfer mechanism, some models of transformer thermal and loss of life will be studied. Thermal mechanisms are complex by their own and even more when applied to a complex system, either geometrically either physically, such as the transformer is. However, the required transformer thermal model must be as simple as possible without losing representative ness of major phenomena involved; a compromise must then be achieved between accuracy and complexity. Based on the thermal model adopted by International Standards, small improvements to increase model accuracy are presented and a comparative study of resulted accuracy under different load and ambient temperature profiles is performed.

Keywords—Modelling thermal parameters, Loss of life models, Transformer thermal.

I. INTRODUCTION

THE purpose of this paper is to analyse the different thermal models proposed in specialised bibliography for oil-immersed distribution transformers as well as their application domain. The usefulness of thermal model is to estimate the highest temperature transformer experiences during its functioning (the hot spot), so that relative ageing rate can be evaluated [2], [3]. Thermal mechanisms are complex by their own and even more when applied to a complex system, either geometrically either physically, such as the transformer is. However, the required transformer thermal model must be as simple as possible without losing representative mess of major phenomena involved; a compromise must then be achieved between accuracy and complexity. For this reason, thermal mechanisms will be simplified, as well as the transformer thermal system itself. Given a few transformer specific parameters, the hot-spot temperature will be estimated as a function of the driving load and ambient temperature. In this paper a brief introduction to transformer involved heat transfer mechanisms is performed, a first simplified thermal model is given and International Standards proposed model as well as respective parameters are presented.

Marius-Constantin Popescu is currently an Associate Professor at the Faculty of Electromechanical and Environmental Engineering, Electromechanical Engineering Department, University of Craiova, ROMANIA, e.mail address popescu.marius.c@gmail.com.

Nikos Mastorakis is currently a Professor in the Technical University of Sofia, BULGARIA, Professor at ASEI (Military Institutes of University Education), Hellenic Naval Academy, GREECE, e.mail address mastor@wseas.org.

Liliana Popescu-Perescu is currently a Teacher in the "E.Cuza" College of Craiova, ROMANIA, e.mail address lpopi2001@yahoo.com

Possible model improvements are derived: the correction of transformer losses due to temperature variation, the convective heat transfer variation with temperature, the existence of a secondary thermal time constant associated to transformer windings and the influence of variable ambient temperature into transformer dynamic thermal system [26], [27].

II.THERMAL MODEL

The heating of a transformer arises from electric and magnetic losses. One can consider the existence of two main active heat sources: the windings and the magnetic core usually referred as windings losses and core functioning losses. Secondary heat losses, in the tank and other metallic parts of the transformer, due to Eddy currents, will be neglected, due to their small proportions. Thermal laws determine that once a thermal gradient is establish, thermal fluxes flow from higher temperature parts to lower ones, until the thermal equilibrium is reached. This heat transition between higher and lower temperature parts can be achieved either by conduction, convection and radiation. Each of these heat transfer mechanisms is dependent upon the materials specific characteristics (thermal capacity, conductivity convection and radiation coefficients), materials anisotropy or isotropy, geometric parameters; some of these characteristics are it self, temperature dependent. The establishment of temperature distribution inside a transformer is very complex and thus, some simplifications must be admitted. Heat transfer from heat sources to cooling medium can be divided into four paths [22], [24]:

- i) from inner parts of the active components (windings and core) to their external surface in contact with oil; here the heat transfer mechanism is mainly due to conductivity;
- ii) from external surfaces of active parts, to oil; here the heat transfer mechanism is mainly due to oil convection;
- iii) from oil to external tank surfaces; neglecting the tank width (where heat transfer is due to conductivity) one can assume that oil convection is the main mechanism of heat transfer;
- iv) from external tank surfaces to external cooling medium (air); here, heat is dissipated by air convection and radiation.

A. Heat transfer mechanisms. Although a transformer is composed of many different parts, its thermal analysis can be started considering the heating general theory of a homogeneous solid body. Heating sources inside a transformer are the windings and the core; both components can be considered solid black bodies, where

conduction is the only mechanism of heat flow [17]. The temperature Θ of an opaque body inside which power losses P_{loss} are generated, is a function of time, t , and spatial references according to [10]:

$$V \left[c_v \frac{\partial \Theta}{\partial t} - \text{div}(\lambda_{th} \overrightarrow{\text{grad}} \Theta) \right] = P_{loss}, \quad (1)$$

where: V - volume [m^3], c_v - thermal capacity per unit volume, at constant pressure [$\text{J m}^{-3} \text{K}^{-1}$], λ_{th} - thermal conductivity [$\text{W m}^{-1} \text{K}^{-1}$] and P_{loss} -power loss [W].

If temperature variations of reduced magnitude are considered, thermal conductivity λ_{th} which, generally, is temperature dependent, can be assumed constant. Therefore, for an anisotropic body presenting different thermal conductivity λ_{thi} for the three main axes x , y and z , equation (1) is given by the Fourier Law [17]:

$$V \left[c_v \frac{\partial \Theta}{\partial t} - \left(\lambda_{thx} \frac{\partial^2 \Theta}{\partial x^2} + \lambda_{thy} \frac{\partial^2 \Theta}{\partial y^2} + \lambda_{thz} \frac{\partial^2 \Theta}{\partial z^2} \right) \right] = P_{loss} \quad (2)$$

If the heating body is considered isotropic ($\lambda_{thx} = \lambda_{thy} = \lambda_{thz} = \lambda_{th}$) and with an infinitely high thermal conductivity, the temperature inside the body will be homogeneous. Thus (2) is reduced to:

$$V c_v \frac{\partial \Theta}{\partial t} = P_{loss}. \quad (3)$$

When the heat generated inside the body is constant, from (3) solution, the temperature evolution with time will lead to an infinite increase of body temperature. In reality, this will not happen as bodies do change thermal energy between each other until a thermal equilibrium is reached,

$\frac{\partial \Theta}{\partial t} = 0$. Considering the changed power between the body and the external surrounding medium, $P_{changed}$, the energy balance at the external surface of the body is:

$$V \left(c_v \frac{\partial \Theta}{\partial t} + P_{changed} \right) = P_{loss}. \quad (4)$$

If the external surrounding medium is a fluid, heat transfer inside it, is mainly due to hot portions of the fluid (in contact with the heating source) which diffuse with cold portions. This mechanism of heat flow due to fluid movements (which can be natural or forced) is denoted as convection. In the mean sense and for small amplitude variations of temperature, Newton defined the rate of heat transferred from a surface A_s of a solid to a fluid, by [4], [18]:

$$P_{con} = (\Theta - \Theta_0) h_{con} A_s \quad (5)$$

where: P_{con} - thermal power transferred by convection [W],

Θ - mean temperature of fluid [$^{\circ}\text{C}$], h_{con} - mean surface convective heat transfer coefficient, excluding radiation [$\text{W m}^{-2} \text{K}^{-1}$] and A_s - body external equivalent refrigeration surface [m^2].

The determination of the mean thermal surface transfer coefficient h_{con} is rather complex; besides being itself temperature and pressure dependent, it is also function of the fluid draining regime (laminar or turbulent), fluid physical characteristics (viscosity, thermal conductivity), draining speed and geometric characteristics of the exchanging surface. For a hot solid body surrounded by a fluid, the fluid draining regime, speed or physical characteristics for all surfaces will hardly be the same, even if the surface temperature can be considered homogeneous. Solid geometric constraints, as the shape of the solid heating body, will always determine "top", "bottom" and "sided" surfaces, relatively to the overall movement of the fluid. For this reason, it is most helpful to employ point or local surface coefficients h_A , defined as:

$$\frac{\partial P_{con}}{\partial A} = (\Theta - \Theta_0) h_A. \quad (6)$$

Generally, the h_{con} value used in (5) is a mean value determined for each specific situation and assumed constant within reduced temperature ranges. Other mechanism through which the body can exchange thermal energy with the external medium is by radiation. Any hot body emits radiant energy that can be absorbed and/or reflected by surrounding bodies at lower temperatures. While conduction and convection are functions of temperature differences, radiation is a function of the fourth power of the body absolute temperature. Stefan empirically stated the basic equation of "black body" thermal radiation that later Boltzmann derived theoretically [21]:

$$P_{rad} = k_{SB} A_s T_{ab}^4, \quad (7)$$

where: P_{rad} - thermal power transferred by radiation [W], k_{SB} - Stefan-Boltzmann constant [$\text{W m}^{-2} \text{K}^{-4}$] and T_{ab} - absolute temperature of the body [K].

Besides the temperature, also this interchange of radiant energy between two bodies is a function of their emissivite, geometry and spatial relative positions. Hottel derived an expression to estimate the power exchanged by radiation, $P_{rad1 \leftrightarrow 2}$ between two surfaces A_{s1} and A_{s2} at absolute temperatures T_1 and T_2 , respectively, being $T_1 > T_2$, [17], [19], [20]:

$$P_{rad1 \leftrightarrow 2} = k_{SB} A_{s1} \mathfrak{F}_{12} (T_1^4 - T_2^4) \equiv \equiv k_{SB} A_{s2} \mathfrak{F}_{21} (T_1^4 - T_2^4), \quad (8)$$

where \mathfrak{F}_{12} and \mathfrak{F}_{21} are functions of the geometry, emissivite and absorption coefficients of the two surfaces. Although heat transfer mechanism models are very well

defined, its application to realistic thermal systems is complex. In most cases, more than one mechanism is involved, real geometric characteristics of bodies are far from ideal ones and hard to be calculated temperature non-homogeneity and parameters dependence upon it, determine complex models with heavy analytical treatments. One of the most elementary thermal models is the homogeneous solid body with infinitive high conductivity, exchanging thermal energy with a surrounded fluid.

From (4) and (5), with $P_{changed} = P_{con}$, one obtains:

$$P_{loss} = Vc_v \frac{\partial \Theta}{\partial t} + (\Theta - \Theta_0) h_{cr} A_s \quad (9)$$

where h_{cr} represents an equivalent heat transfer coefficient taking account of convection and radiation.

Assuming that only the hot body temperature, Θ , is time dependent and that initial condition is for $t=0 \Rightarrow \Theta = \Theta_0$, the resolution of (9) yields to [5], [10]:

$$\Theta(t) = \Theta_0 + \frac{P_{loss}}{h_{cr} A_s} [1 - e^{(-t/\tau)}]. \quad (10)$$

Its equivalent thermal time constant denoted by τ , is given by,

$$\tau = \frac{Vc_v}{h_{cr} A_s} = \frac{c_m M}{h_{cr} A_s}, \quad (11)$$

where M [kg] is the mass of the body and c_m is the thermal capacity per unit mass, at constant pressure [$J \text{ kg}^{-1} \text{ K}^{-1}$].

The thermal time constant is a measure of the system thermal inertia and presents a geometric factor given by [6], [8]

$$\frac{V}{A_s} \text{ or } \frac{M}{A_s} \quad (12)$$

and a thermal factor given by

$$\frac{c_v}{h_{cr}} \text{ or } \frac{c_m}{h_{cr}}. \quad (13)$$

For a body of volume V , its thermal time constant will increase with its thermal capacity (measuring/reflecting its ability to store thermal energy) but will/decrease with its equivalent refrigerating surface A_s , well as with its refrigeration efficiency (represented by the transfer coefficient h_{cr}). These last two parameters are, as referred before, very difficult to quantify in real systems. However, the thermal time constant is a very useful concept due to its physical interpretation and its quasi-invariance; variability of parameters M , c_m , c_v , h_{cr} and A_s are frequently correlated and resultant variability of τ is practically negligible. Denoting by $\Delta\Theta_f$ the body final

temperature rise when the steady-state regime is reached, it is:

$$\Delta\Theta_f = \frac{P_{loss}}{h_{cr} A_s}. \quad (14)$$

Inserting (14) into (11) one obtains [5], [13]:

$$\tau = Vc_v \frac{\Delta\Theta_f}{P_{loss}} = Mc_m \frac{\Delta\Theta_f}{P_{loss}}, \quad (15)$$

which is a most helpful expression since it relates quantities of easy determination and, for the specific case of transformers, usually obtained from manufacturing heating tests?

The transformer thermal time constant and final temperature increments are major subjects of this work so the theme will be recovered several times along this exposition.

B. Transformer simplified thermal model. The complexity of realistic thermal systems imposes some simplifications to obtain suitable thermal models. In this section, a simplified oil-immersed transformer thermal model will be presented. The transformer is divided into three major components: core and windings assembly, denoted by the subscript "c", oil, denoted by the subscript "o", and tank, denoted by the subscript "t". No radiators or fans are considered since, generally [25], they are not used on distribution transformers. If existing, it is possible to adjust the equivalent exchange coefficient in order to traduce their effect. Each of these components is assumed to be isotropic in all directions, with infinitely high thermal conductivity. Under this condition, no thermal gradient exists inside each component. Temperatures determined from the model can be considered as the equivalent average temperatures of each component.

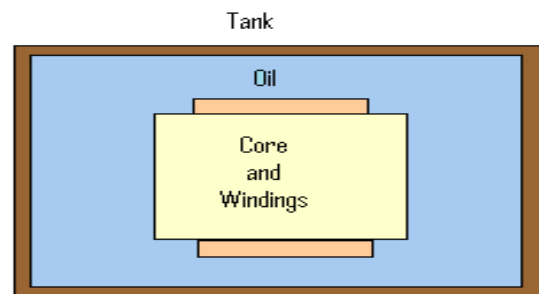


Fig. 1: Temperature distribution diagram of an oil filled transformer.

The assembly of core and windings is justified with the fact of both being solid materials (conduction is the only thermal mechanism involved) although thermal properties reflect some differences, mainly in windings made up of copper or aluminium and in magnetic sheets thermal conductivity depending on orientation (Table 1). Considering the core and windings assembly as a homogeneous body where power losses P_{loss} are generated, the energy balance at its surface, is traduced by

the equation [14]:

$$P_{loss} = [Vc_v]_c \frac{\partial T_c}{\partial t} + (T_c + T_0)[h_{con}A_s]_c \quad (16)$$

Similarly, the energy balance at the tank internal surface leads to:

$$(T_c + T_0)[h_{con}A_s]_c = [Vc_v]_0 \frac{\partial T_c}{\partial t} + (T_0 - T_t)[h_{con}A_s]_t \quad (17)$$

and at tank external surface:

$$(T_0 - T_t)[h_{con}A_s]_t = [Vc_v]_c \frac{\partial T_t}{\partial t} + (T_t - T_a)[h_{con}A_s]_t + k_{SB}A_t \mathfrak{F}_{t \leftrightarrow a} (T_t^4 - T_a^4) \quad (18)$$

where T_a denotes the absolute average temperature of the ambient air at transformer surroundings and $\mathfrak{F}_{12 \ t \leftrightarrow a}$ is a function of tank and air absorption coefficients, emissivity and tank geometry, which determination is rather complex.

Table 1: Physical values of core and winding materials at averaging operating temperatures of electrical machinery [9].

Material	Direction	Specific mass m_v [kg.m ⁻³]	Specific thermal capacity per unit mass C_m [J.kg ⁻¹ K ⁻¹]	Specific thermal capacity per unit volume $C_v = m_v C_m$ [kJ.m ⁻³ K ⁻¹]	Thermal conductivity λ_{th} [W.m ⁻¹ K ⁻¹]
Magnetic	Longitudinal				1,1
		7 650	460	3519	
	Transversal				27
Copper		8 900	398	3542	384
Aluminium		2 700	879	2373	204

Although the transformer has already been reduced to three major components in order to simplify its thermal model, the temperature dependence of some parameters such as thermal coefficients h_{con} and specific thermal capacities c_v , determine the use of a numerical method to solve the equation system. Some extended work about thermal coefficients and dependence with temperature of specific thermal capacities can be found on [1].

III. THERMAL MODELS COMPARATIVE STUDY

In order to study the application domain and the impact of transformer thermal model improvements presented, some simulations were performed. First, each effect was analysed separately and then joined effects were considered [15], [16]. To simplify graphical notations and nomenclature the following models and respective sigma

will be referred on next sections.

Reference Model, referred on graphs as "Ref", is the model proposed by International Standards [11], [12].

Resistance Model, referred on graphs as "Res", is based on Reference model but introducing the resistance correction factor $C(\Theta_{hs})$ on top-oil and hot-spot steady-state temperature rises.

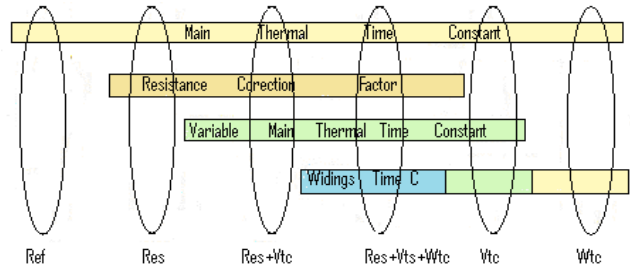


Fig. 2: Analysed aspects and models.

Variable time constant Model, referred on graphs as "Vtc", is based on Reference model where the time constant variation with top-oil temperature rises was considered.

Windings time constant Model, referred on graphs as "Wtc", is based on Reference model but where windings time constant was introduced.

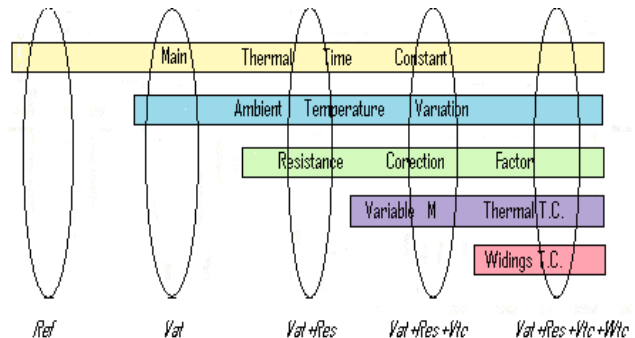


Fig. 3: Analysed aspects and models "joined" with "Vat" model.

Variable Ambient Temperature Model, referred on graphs as "Vat", is based on Reference model but considering variable ambient temperature into the transformer dynamics [27].

The following models will simulate the "joined" effects: "Res+Vtc" model takes into consideration both the resistance correction factor and variable time constant. The "Res+Vtc+Wtc" model considers the effect introduced by the windings thermal time constant, to the previous "Res+Vtc" model. Similar joined models are built, relatively to "Vat" model (Fig. 3).

A. Load profiles and transformer parameters. The results presented were obtained considering a distribution transformer rated 630 kVA, 10 kV/400 V with copper windings [23]. When parameters used on the relevant expressions were unknown, those proposed on [12] were used:

Table 2: Transformer Specific Parameters

$\Delta\Theta_{OR} = 55K$	$\Delta\Theta_{hsR} = 23K$	$\Theta_{ref} = 75^{\circ}C$
$n = 0.8$	$R = 5 p.u. \text{ at } 75^{\circ}C$	$L = 0.05 p.u. \text{ at } 75^{\circ}C$
$\tau_0 = 3 \text{ hours}$	$\tau_w = 1/12 \text{ hours (i.e. 5 min)}$	$T_o = 235 K$

Except for section §3.3 ambient temperature was assumed to be constant and equal to 20°C. In order to emphasise alterations introduced by each model improvement, simulation programs use 3 normalised 24 hours load cycles represented, as general, in Figure 4. These fictitious load cycles were defined in order to cover the most of possible situations and to overstate the influence of parameters and models.

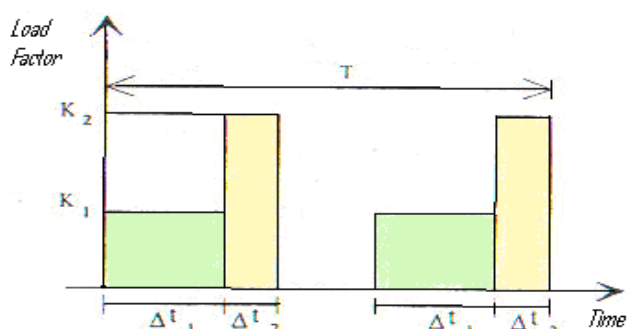


Fig. 4: General Load Cycle used in computer simulation.

Each of the three load cycles is specified as follows, according to the notation of Figure 4.

Table 3: Load Cycles Specification.

Load Cycle	$T[h]$	K_1	$\Delta t_1/T$	K_2	$\Delta t_2/T$
n°1	24	0.4	1/8	1.2	1/8
n°2	24	1.0	1/2	0	1/2
n°3	24	0.7	3/40	1.4	1/120

As initial condition of the simulations, the transformer was assumed to be disconnected from power supply and at ambient temperature (i.e. long term steady-state). For this reason, a 48 hours simulation was used. Presented graphs are then referred to last 24 hours, as the thermal transient must be practically extinguished, ($\tau_0/T=1/8$). The load cycle n°1 is a 6 hours periodic overload, with unity cyclic ratio (duty cycle); n°2 is 24 hours periodic no load - rated load, with unity cyclic ratio (duty cycle) and n°3 is 2 hours periodic impulsive overload, with 1/10 cyclic ratio. On load cycle n°2 $K_2=0$ p.u. means that the transformer is disconnected from power supply and so both load and no-load losses are null [20].

B. Simulated load profiles under constant ambient temperature. "Resistance" Model - Figure 5 represents "Ref" and "Res" models steady-state hot-spot temperature for permanent 24 hours loads and for different values of

ratio L (Additional to DC Loss Ratio). Below 100°C, differences between "Res" and "Ref" models are almost imperceptible. Provided hot-spot temperatures are below 75°C, the influence of the resistance correction factor on loss of life calculations is almost insignificant. On the other hand, above 75°C, hot-spot temperature estimated by the "Resistance" model increases significantly. Neglecting resistance correction factor C is traduced to very different values of loss of life since V_{ag} is very sensitive to high values of hot-spot temperature Θ_{hs} . Moreover, the correction introduced by the resistance factor becomes more pertinent as the ratio additional / DC losses, L, decreases, since additional losses variation counteracts the DC losses increase with temperature (Fig. 5). Under a reduced L value and due to its major proportion, the overall effect is imposed by DC losses.

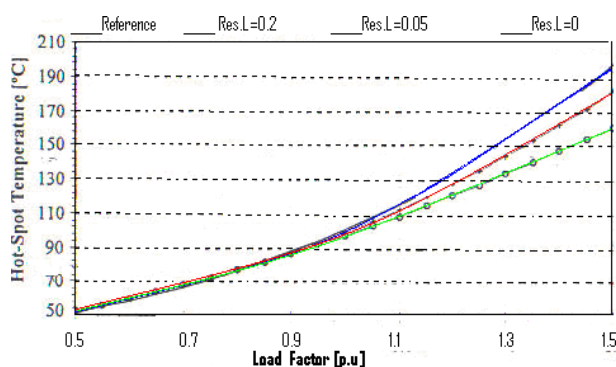


Fig. 5: Influence of resistance correction factor (steady state).

Since the C factor depends upon the unknown hot-spot temperature, its value will be estimated one calculation step behind, i.e., hot-spot temperature estimated in calculation step t will use factor C estimated in step t-1. Figure 6 represents obtained hot-spot temperatures for "Reference" and "Resistance" models, under load cycle n°1. Factor C is also represented on the same figure. As temperatures overpass 75°C, factor C becomes larger than unity, increasing differences btluwxn the hot-spot temperatures of "Reference" and "Resistance" models (i.e. Fig.6). Analytically, differences between both models are due to estimated steady-state temperatures. Has difference is relevant mainly, for overload $K=1.2$ p.u. which is well traduced by the step variation of C factor (Fig. 6).

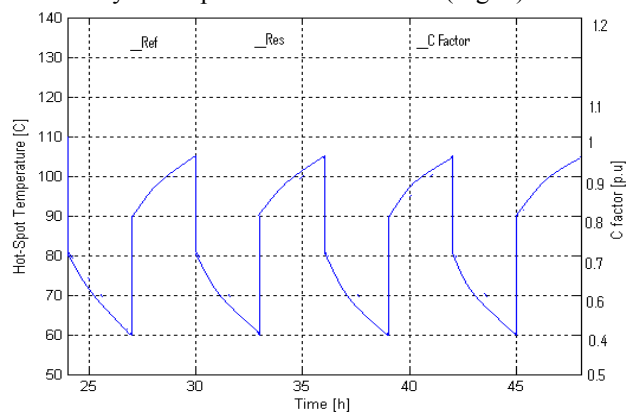


Fig. 6: Influence of resistance correction factor.

Since this C factor is not fixed within each step but readjusted for each time increment, it's increasing with heating periods, and with cooling ones, can also be observed. The C factor influence on estimated loss of life, is not directly dependent upon overload duration (as will happen with the "Windings time constant" model) but most of all, upon reached hot-spot temperatures. One can conclude that C factor should be use, every time hot-spot temperatures above 75°C are expected to be reached [23].

"Variable Time Constant" Model - To test the influence of the main thermal time constant over hot-spot temperature, load cycle n°2 was simulated and models "Reference" and "Variable time constant" were compared. Just before loading, transformer is assumed to be disconnected from power supply and at ambient temperature (20°C).

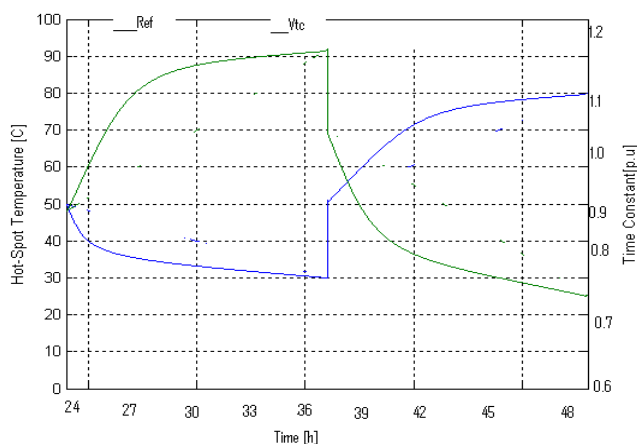


Fig. 7: Influence of variable time constant.

Figure 7 represents hot-spot temperatures and the $\tau_0 (\Delta\Theta_o)/\tau_0$ function. Variation introduced by, "speeds up" heating process and as much, as severe is the overload; cooling period tends to follow the "Reference" model. The variation of transformer thermal time constant reflects the variation in the convective heat transfer coefficient with temperature differences between transformer external surface and surrounding air. As expected, its effect is as stronger as severe is the overload, since higher temperature differences are reached. Under this load cycle, final estimated τ_0 decreasing during heating period is about 20% of its rated value ($\tau_0=3$ hours); but this value increased 35% when this same load cycle was simulated with an overload of 2 p.u. (i.e., on load cycle n°2, $K_1=2$ p.u.) and only 9% for an overload of 0.5 p.u. (i.e., on load cycle n°2, $K_1=0.5$ p.u.). Relatively to the cooling period (12 hours), the transformer thermal time constant increased about 10% of its rated value, meaning a variation amplitude, from the hottest temperature (reached at 12 hours) until the coldest (reached at 24 hours), of about 30% of its rated value. If the overload duration is much longer than the transformer main thermal time constant, the reached hot-spot temperatures simulated by "Ref" and "Vtc" models are similar. For overloads, the difference increases and is maximal when the overload duration is of magnitude as transformer main thermal time constant [27].

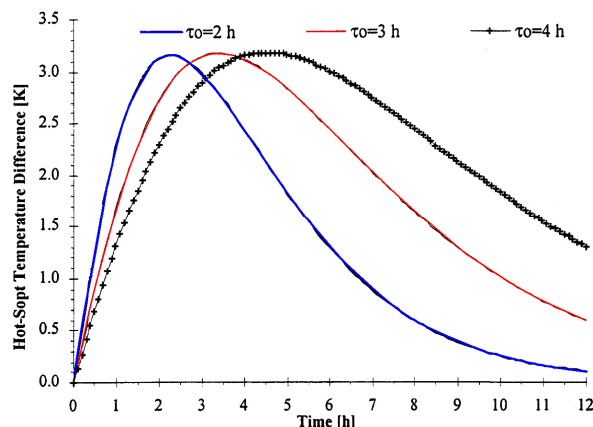


Fig. 8: Hot-spot differences between *Ref* and *Vtc* models under load cycle n°2 and for 3 different transformer main thermal time constants.

Figure 8 represents differences between "Ref" and "Vtc" models simulated under load cycle n°2, considering 3 fantail values for the transformer main thermal time constant. While for overloads of reduced magnitude (i.e. load cycle n°3) hot-spot differences between models are imperceptible and have no impact on loss of life values, for longer overloads, and although differences on final reached hot-spot temperature are also imperceptible, the consideration of the overall overload period, will, clearly, be reflected on loss of life. From the above simulations, it can be concluded that larger differences introduced by variation of the main thermal time constant, are verified for severe overloads with duration similar or longer than the nominal value of the main thermal time constant.

C. Realistic load profile under ambient temperature.
The previous simulation cycles explore particular aspects of each model; in order to get a global view, simulations were carried over a realistic load profile, obtained from the Romania power supply company (EDP). It is an essentially residential profile, from a neighbourhood city near Craiova and refers to the 27 December 2005, selected at random. Peak point load factor is $K \approx 1.32$ p.u. reached at 8 p.m. and minimum load factor is $K \approx 0.53$ p.u. at 7 a.m.. Available data measurements were made each half an hour. All load cycle simulations presented till now, assumed a constant ambient temperature of 20°C . For this realistic load profile, the available data did not include the correspondent "real" ambient temperature variation, but only the daily maximum ($\Theta_M=11^{\circ}\text{C}$) and minimum ($\Theta_m=5^{\circ}\text{C}$) temperatures. The available data included only the ambient temperature when peak load factor point was reached: about 9.6°C . Three situations were then considered [3], [19]:

i) the constant ambient temperature corresponding to the temperature arithmetic mean

$$\Theta_a(t) = \overline{\Theta_a} \quad \text{with} \quad \overline{\Theta_a} \equiv \frac{\Theta_M + \Theta_m}{2}, \quad (19)$$

ii) the daily sinusoidal variation of ambient temperature, so that 9.6°C would be reached at 8 p.m..

With t [h] and t_0 presenting a phase at origin, it will be:

$$\Theta_a(t) = \overline{\Theta}_a - \Delta\Theta_a \sin\left[\frac{2\pi}{24}(t+t_0)\right]$$

with
$$\Delta\Theta_a \equiv \frac{\Theta_M + \Theta_m}{2}, \quad (20)$$

iii) the weighted ambient temperature

$$\Theta_a(t) = \Theta_{aE}. \quad (21)$$

According to ambient temperature data, it must be:

$$\overline{\Theta}_a = 8^\circ\text{C}, \quad \Delta\Theta_a = 6^\circ\text{C} \quad \text{and} \quad t_0 = 2\text{h} \quad (22)$$

The sinusoidal ambient temperature, the weighted ambient temperature and the realistic load profile used in simulations are represented on Figure 9.

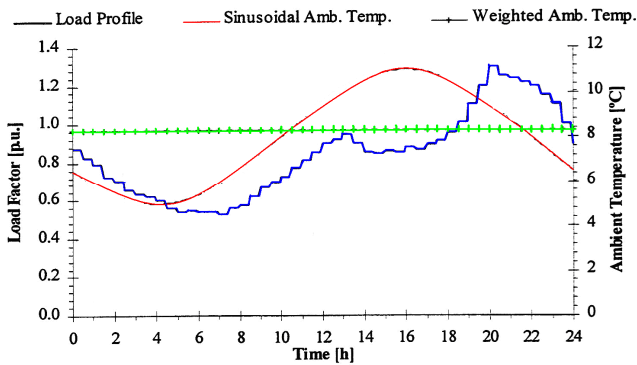


Fig. 9: Realistic load and ambient temperature profiles.

Figure 10 shows hot-spot temperatures obtained with each of the studied thermal models. To preserve figure clarity, only the peak period is represented because differences between models out of it, could hardly be distinguished. Once again, "Ref" model revealed to be the most conservative one and differences between models rise, when load factor is above 1 p.u. These results show that the correlation degree, between load and ambient temperature profiles, do have influence on reached hot-spot temperatures and, by consequence, on life expectancy results [28].

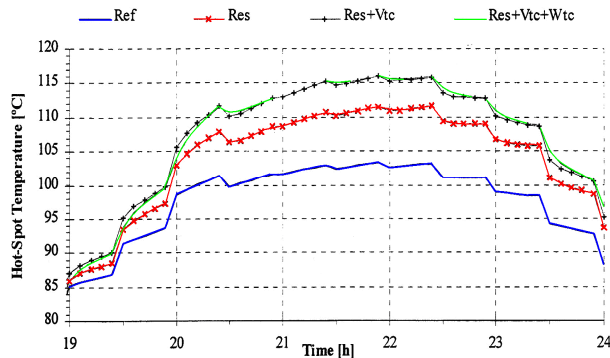


Fig. 10: Hot-spot temperature assuming sinusoidal variation of ambient temperature.

Table 4 represents the maximum hot-spot temperatures for "Ref" model and the differences between the other three models and this one, reached under the three considered ambient temperature profiles. For loss of life calculations under variable profiles, the knowledge of maximum reached hot-spot temperature is not sufficient since, being the load profile a variable one, the all period under analysis (1 day, in this case), must be considered.

Table 4: Maximum hot-spot temperature differences between models.

Ambient Temperature	Ref [K]	Res [K]	Res+Vtc [K]	Res+Vtc+Wtc
Arithmetic	103.5	+8.3	+12.5	+12.6
Sinusoidal	103.3	+8.3	+12.7	+12.7
Weighted	103.8	+8.4	+12.6	+12.7

Daily loss of life values are represented on Figure 10. The values relative to arithmetic ambient temperature are systematically below those obtained with sinusoidal and weighted ambient temperature. Attending to weighted ambient temperature definition (§2) loss of life values calculated under a sinusoidal or a weighted ambient temperature should be similar as, in fact are. This similitude, however, is erroneous; from definition, the application domain of weighted ambient temperature is restricted to constant loads, which is not the case under analysis.

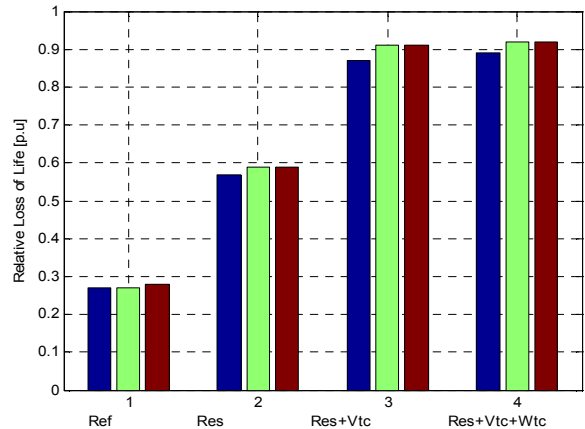


Fig. 10: Relative loss of life for a 24 hours period under reduced ambient temperature amplitude ($\Delta\Theta_a=6\text{K}$).

D. The weighted ambient temperature. Figure 11 represents the loss of life values obtained for the same realistic load profile but under a much wide ambient temperature profile, meaning a wider ambient temperature range; Figure 11 values were obtained with $\Delta\Theta_a=16^\circ\text{C}$ and for the same arithmetic mean ($\overline{\Theta}_a=8^\circ\text{C}$). Under this wide ambient temperature profile, differences between loss of life obtained with sinusoidal and weighted ambient temperature became visible. The reason for these differences reside on the International Standards definition of weighted ambient temperature; weighted ambient

temperature do lead to the same loss of life of an equivalent sinusoidal variation, but uniquely under constant load profiles, which is not the case of simulations represented on Figure 10 and Figure 11. To deeply analyse this fact, errors between loss of life values obtained with a sinusoidal profile and a weighted ambient temperature, as a function of ambient temperature range, were studied. Two simulation sets were performed: one considers the realistic load profile; the other assumes a constant rated load ($K=1$ p.u.). Also two arithmetic mean values for ambient temperature were assumed: $\bar{\Theta}_a=10^\circ\text{C}$ and $\bar{\Theta}_a=20^\circ\text{C}$.

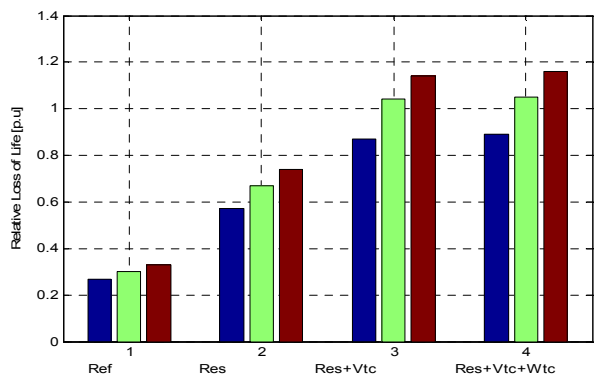
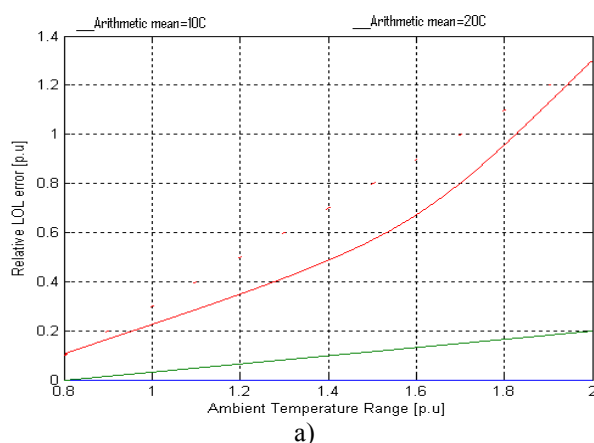


Fig. 11: Relative loss of life for a 24 hours period under wide ambient temperature amplitude ($\Delta\Theta_a=16\text{K}$).

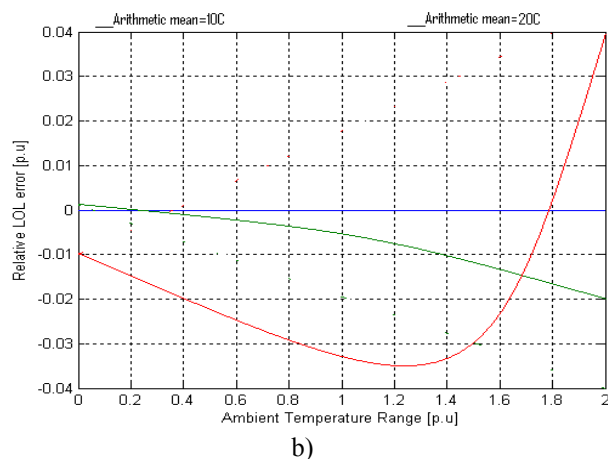
Errors between loss of life values obtained under sinusoidal load profile and weighted ambient temperature, are plotted as a function of ambient temperature range. These ranges are in per unit values of the respective arithmetic means. Loss of life ranges are referred to loss of life obtained under constant ambient temperature ($\Theta_a(t)=\bar{\Theta}_a$). Results were obtained with the "Reference" model and are represented on Figure 12. Loss of life errors are defined as:

$$LOL_{error} = LOL_{weighted} - LOL_{sinusoidal} \quad (23)$$

From Figure 12 one concludes that the error magnitude under realistic load profile is much greater than that under constant load [30].



a)



b)

Fig. 12: Loss of Life errors between sinusoidal and weighted ambient temperature (a) under a realistic load (b) under a constant load.

Moreover, under realistic load, the error increases with ambient temperature range as well as with its arithmetic mean. The very same set of variable ambient and load profiles, leads to completely different values of loss of life, depending upon the correlation between them. Loss of life will be maximum if both load and ambient temperature peak values are reached simultaneously and minimum if load peak is reached at minimal ambient temperature.

E. "Variable ambient temperature" model. With the previous analysed models, any change in ambient temperature will be instantaneously reflected on top-oil temperature rise and, consequently, on transformer loss of life. Figure 13 represents hot-spot temperatures for the realistic load profile, under sinusoidal, arithmetic and weighted ambient temperature profiles, simulated by the "Reference" model. It is clear the instantaneous effect of sinusoidal ambient temperature variation over top-oil temperature and consequently, relative ageing rate; sinusoidal ambient temperature becomes lower than constant ones around 10 p.m., which is instantaneously traduced by a correspondent lower hot-spot temperature.

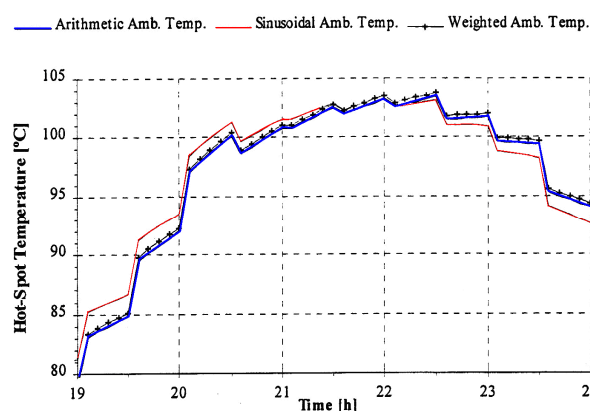


Fig. 13: Hot-Spot temperature for constant, weighted and sinusoidal ambient temperature under "Ref" model.

This is due to the fact that "Reference" model does not consider transformer dynamic behaviour due to ambient

temperature variations. Maximum reached hot-spot temperatures are represented on Table 5 and on Figure 14, its evolution for the peak load period.

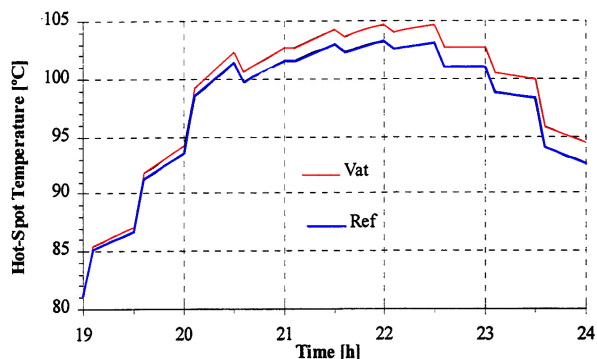


Fig. 14: Hot-spot temperatures for "Ref" and "Vat" models under sinusoidal ambient temperature.

Table 5: Maximum hot-spot temperature for "Ref" and "Vat" models.

Ambient Temperature	Ref [°C]	Vat [°C]
Sinusoidal	103.3	104.7

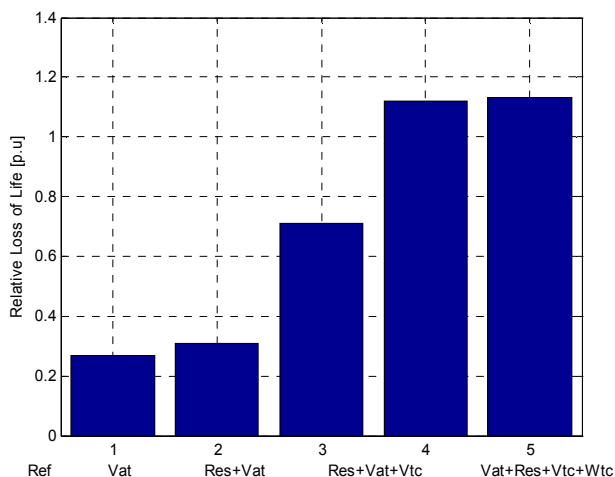


Fig. 15: Relative 24 hours period loss of life, considering "Vat" model.

Figure 15 represents daily loss of life considering "Vat" and additional models. The single effect of ambient temperature variation leads to an increase in transformer loss of life. This is so, because transformer will react to the 10 a.m. to 10 p.m. increase in ambient temperature, with a delay associated to its thermal time constant (Figure 14). Simultaneously, the variable load is increasing, and higher hot-spot temperatures will be reached. If subsequent models "Vat+Res", "Vat+Res+Vtc" and "Vat+Res+Vtc+Wtc" are considered, loss of life will increase more than 4 times relatively to the value obtained with the "Reference" model. This loss of life increase with ambient temperature variation is expected to assume larger values, if industrial load profiles and/or unfavourable temporal correlation between load and ambient temperature profiles are considered.

IV. SIMULATIONS

This demonstration illustrates the use of the linear transformer to simulate a three-winding distribution transformer rated 75 kVA - 14400/120/120 V (Fig. 16). The transformer primary is connected to a high voltage source (14,400 V rms). Two identical inductive loads (20 kW -10 kvar) are connected to the two secondaries [29].

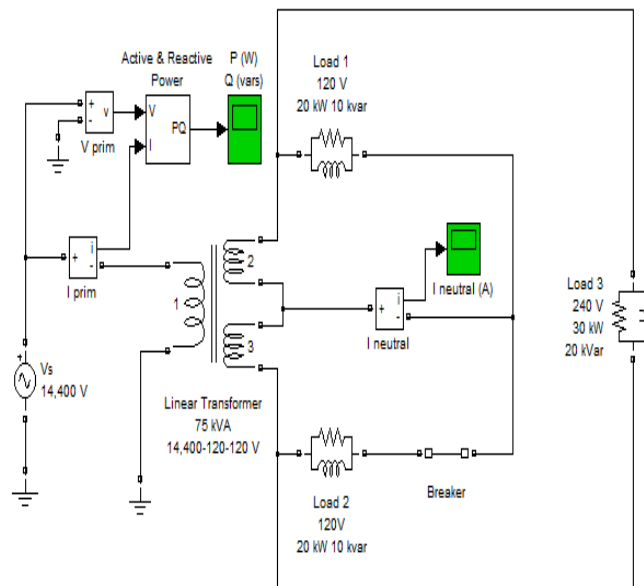


Fig. 16: Linear transformer by Simulink.

A third capacitive load (30 kW -20 kvar) is fed at 240 V. Initially, the circuit breaker in series with Load 2 is closed, so that the system is balanced. Open the powergui block to obtain the initial voltage and current phasors in steady state.

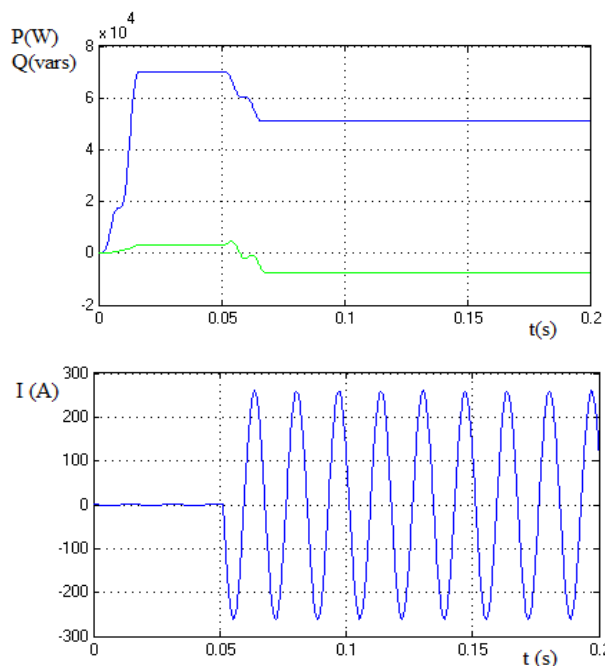


Fig. 17: Parameters transformer.

As loads are balanced the neutral current is practically zero. Furthermore, as the inductive reactive power of Load 1 and Load 2 (2×10 kvar) is compensated by the capacitive reactive power of Load 3 (20 kvar), the primary current is almost in phase with voltage. The small phase shift (-2.8 deg.) is due to the reactive power associated with transformer reactive losses. Open the two scopes and start the simulation. The following observations can be made: when the circuit breaker opens, a current starts to flow in the neutral as a result of the load unbalance. The active power computed from the primary voltage and current is measured by a Simulink block which can be found in the Extras/Measurement library. When the breaker opens, the active power decreases from 70 kW to 50 kW. This demonstration (Fig.18) illustrates measurement distortion due to saturation of a current transformer (CT).

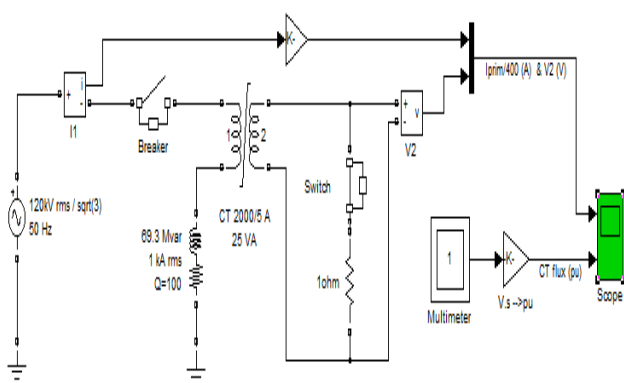


Fig. 18: Current Transformer Saturation by Simulink; in order to observe CT saturation, change the Breaker closing time to $t=1/50$ sec (1 cycle).

A current transformer (CT) is used to measure current in a shunt inductor connected on a 120 kV network. The CT is rated 2000A/5A, 5 VA. The primary winding which consists of a single turn passing through the CT toroidal core is connected in series with the shunt inductor rated 69.3 Mvar, 69.3 kV ($120\text{kV}/\sqrt{3}$), 1 kA rms [29].

The secondary winding consisting of $1 \times 2000/5=400$ turns is short circuited through a 1 ohm load resistance. A voltage sensor connected at the secondary reads a voltage which should be proportional to the primary current. In steady state, the current flowing in the secondary is $1000 \times 5/2000=2.5$ A (2.5 Vrms or 3.54 Vpeak read by the voltage measurement block V2).

Open the CT dialog box and observe how the CT parameters are specified. The CT is assumed to saturate at 10 pu and a simple 2 segment saturation characteristic is used. The primary current reflected on the secondary and the voltage developed across the 1 ohm resistance is sent to trace 1 of the Scope block. The CT flux, measured by the Multimeter block is converted in pu and sent to trace 2. The switch connected in series with the CT secondary is normally closed. This switch will be used later to illustrate over voltages produced when CT secondary is left open.

Normal operation. In this test, the breaker is closed at a peak of source voltage ($t=1.25$ cycle). This switching

produces no current asymmetry. Start the simulation and observe the CT primary current and secondary voltage (first take of Scope block). As expected the CT current and voltage are sinusoidal and the measurement error due to CT resistance and leakage reactances is not significant. The flux contains a DC component but it stays lower than the 10 pu saturation value.

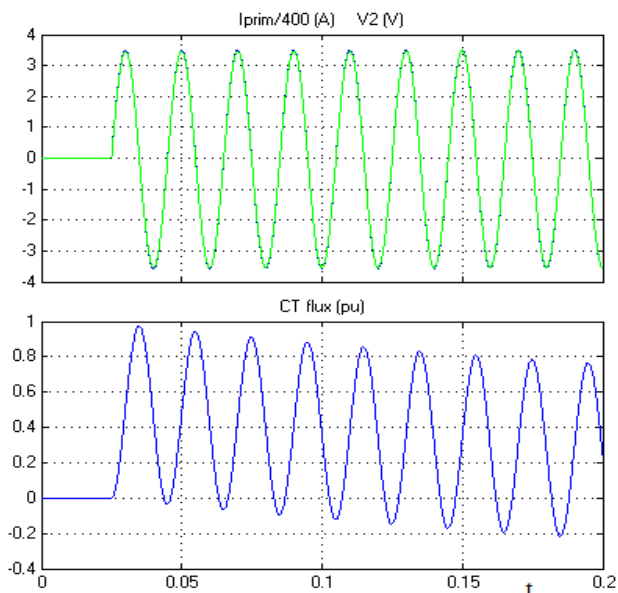


Fig. 19: Parameters transformer
 (1pu flux= $0.0125\text{V} \times \sqrt{2}/(2 \times \pi \times 50)=5.63 \times 10^{-5}$ V.s)

CT saturation due to current asymmetry. Now, change the breaker closing time in order to close at a voltage zero crossing. Use $t=1/50$ s. This switching instant will now produce full current asymmetry in the shunt reactor. Restart the simulation. Observe that for the first 3 cycles, the flux stays lower than the saturation knee point (10 pu). The CT voltage output V2 then follows the primary current. However, after 3 cycles, the flux asymmetry produced by the primary current causes CT saturation, thus producing large distortion of CT secondary voltage.

Over voltage due to CT secondary opening. Reprogram the primary breaker closing time at $t=1.25/50$ s (no flux asymmetry) and change the secondary switch opening time to $t=0.1$ s. Restart the simulation and observe the large over voltage produced when the CT secondary is opened. The flux has a square wave shape chopped at +10 and -10 pu. Large $d\phi/dt$ produced at flux inversion generates high voltage spikes (250 V).

V. CONCLUSIONS

This paper has shown definitive improvements on the transformer thermal model, relatively to the International Standards model. Maximal hot-spot temperatures and relative loss of life, obtained with International Standards model may be underestimated when transformer operates under larger and severe overloads and with unfavourable temporal correlation between load and ambient temperature. For severe and of very short duration overloads, neglecting windings thermal time constant can

lead to overestimation of transformer loss of life, since the thermal filtering effect is not taken into consideration. For this kind of load cycles, the insulation thermal loss of life criterion will lead to different conclusions relatively to maximum windings temperature criterion would. When a realistic ambient temperature of sinusoidal profile can be assumed, the use of ambient arithmetic mean does lead to loss of life underestimation and the weighted ambient temperature can lead to important overestimation, mainly for varying load profiles under higher and of wide range ambient temperature profiles. Due to temporal correlation between loads and ambient temperature, continuously varying profiles are almost indispensable when loads or temperature ranges are wide or arithmetic it presents considerable values. From the simulations performed in this paper, it can be concluded that larger differences introduced by variation of the main thermal time constant, are verified for severe overloads with duration similar or longer than the nominal value of the main thermal time constant.

REFERENCES

- [1] Alegi G., Black W., "Real-Time Thermal Model for on Oil-Immersed Forced Air Cooled Transformer", IEEE Transactions on Power Delivery, Vol. 5, n^o2, April 1990.
- [2] Aubin J., Bergeron R., Morin R., "Distribution Transformer Overloading Capability Under Cold-Load Pickup Conditions", IEEE Transactions on Power Delivery, Vol. 5, n^o4, pp.1883-1891, November 1991.
- [3] Aubin J., Langhame Y., "Effect of Oil Viscosity on Transformer Loading Capability at Low Ambient Temperature", IEEE Transactions on Power Delivery, Vol. 7, n^o2, pp.516-524, April 1992.
- [4] Boteanu N., Popescu M.C., Manolea Gh., Petrisor A. "Dynamic of Electrical Drive Systems with Heating Consideration", International Journal of Mathematical Models and Methods in Applied Sciences, Issue 3, Vol.3, pp.299-308, 2009.
- [5] Boteanu N., Popescu M.C., Ravigan F., "Energetic Optimization with Arbitrary Terminal Moment of Electric Drives Systems", International Journal of Mathematical Models and Methods in Applied Sciences Issues 3, Vol.2, pp.393-402, 2008.
- [6] Brancato E.L., Insulation Aging: An Historical and Critical Review, IEEE Transactions on Electrical Insulation, Vol. 13, n^o4, pp. 308-317, August 1978.
- [7] Dakin T.W., "Electrical Insulation Deterioration Treated as a Chemical Rate Phenomenon", AIEE Transaction, Vol. 67, pp.113-122, 1948.
- [8] Ilie F., Bulucea C.A., Popescu M.C., "Simulations of Oil-filled Transformer Loss-of-Life Models", Proceedings of the Applied Computing Conference, Published by WSEAS Press, pp.195-202, Vouliagmeni Beach, Greece, September 2009.
- [9] Heuillard J.F., "Refroidissement des Machines Tournantes", Techniques de l'Ingenieur, Serie D, Genie Electrique, D447, D448, D449.
- [10] IEC-76, Part 1, International Electrotechnical Commission, Power Transformers Temperature Rise, Second Edition, 1993.
- [11] IEC-76, Part 2, International Electrotechnical Commission, Power Transformers Temperature Rise, Second Edition, 1993.
- [12] IEC-354, International Electrotechnical Commission, Loading Guide for Oil-Immersed Power Transformers, Second Edition, 1991.
- [13] Kalic D., Radakovic Z., Lazarevic Z., Radosavljevic R., "On the determination of characteristic temperatures in power oil transformers during transient states", Archiv fur Electrotechnik, n^o76, pp.457-468,1993.
- [14] Lahoti B.D., Flowers D.E., "Evaluation of Transformer Loading above Nameplate Rating", IEEE Transactions on Power Apparatus and Systems, Vol. 100, n^o4, pp.1989-1998, 1981.
- [15] Lesieutre B.C., Hagman W.H., Kirtley L., "An Improved Transformer Top Oil Temperature Model for Use in An On-Line Monitoring and Diagnostics System", IEEE Transaction on Power Delivery, Vol. 12, n^o1, pp. 249-256, 1997.
- [16] Lindsay J.F., "Temperature Rise of an Oil-Filled Transformer with Varying Load", IEEE Transactions on Power Apparatus and Systems, Vol. 103, n^o9, pp.2530-2535, September 1984.
- [17] Mastorakis N., Bulucea C.A., Popescu M.C., Manolea Gh., Perescu L., "Electromagnetic and Thermal Model Parameters of Oil-Filled Transformers", WSEAS Transactions on Circuits and Systems, Issue 6, Volume 8, pp.475-486, June 2009.
- [18] Mastorakis N., Bulucea C.A., Manolea Gh., Popescu M.C., Perescu-Popescu L., "Model for Predictive Control of Temperature in Oil-filled Transformers", Proceedings of the 11th WSEAS International Conference on Automatic Control, Modelling and Simulation, pp.157-165, Istanbul, Turkey, May- June 2009.
- [19] Mastorakis N., Bulucea C.A., Popescu M.C., "Transformer Electromagnetic and Thermal Models", 9th WSEAS International Conference on Power Systems: Advances in Power Systems, pp.108-117. Budapest, Hungary, September 3-5, 2009.
- [20] Mastorakis N., Popescu M.C., Bulucea C.A., "Analysis in Time-Frequency Domain of Asynchronous Motors Control with Inverter Switching at Zero Voltage", Proceedings of the 8th WSEAS International Conference on Education and Educational Technology: Advanced Educational Topics and Technologies, pp.126-132, Published by WSEAS Press Genova, October 2009.
- [21] Nicola D.A., Bulucea C.A., Cismaru D.C., Brandusa C., Manolea Gh., Popescu M.C., "Energy Saving in Electric Trainswith Traction Induction Motors", Proceedings of the 4th IASME/WSEAS International Conference on Energy & Environment, pp.226-231, Cambridge, February 2009.
- [22] Pierce L.W., Predicting Liquid Filled Transformer Loading Capability, IEEE Transactions on Industry Applications, Vol. 30, n^o1, January/February 1994.
- [23] Pierrat L., Resende M.J., Santana J., "Power Transformers Life Expectancy Under Distorting Power Electronic Loads", IEEE International Symposium on Industrial Electronics, Warsaw, Poland, pp.578-583, 1996.
- [24] Popescu M.C., Mastorakis N., Bulucea C.A., Manolea Gh., Perescu L., "Non-Linear Thermal Model for Transformers Study", WSEAS Transactions on Circuits and Systems, Issue 6, Vol.8, pp.487-497, June 2009.
- [25] Popescu M.C., Manolea Gh., Bulucea C.A., Boteanu N., Perescu-Popescu L., Muntean I.O., "Transformer Model Extension for Variation of Additional Losses with Frequency", Proceedings of the 11th WSEAS International Conference on Automatic Control, Modelling and Simulation, pp.166-171, Istanbul, Turkey, May June 2009.
- [26] Popescu M.C., Mastorakis N., Bulucea C.A., Manolea Gh., Perescu L., "Non-Linear Thermal Model for Transformers Study", WSEAS Transactions on Circuits and Systems, Issue 6, Vol.8, pp.487-497, June 2009.
- [27] Popescu M.C., Petrişor A., Drighiciu M.A., "Modelling and Simulation of a Variable Speed Air-Conditioning System", International Conference on Automation, Quality and Testing, Robotics, Proceedings pp.175-181, Cluj-Napoca, May 2008.
- [28] Saha T.K., Darveniza M., Hill D.J.T., Le T.T., "Electrical and Chemical Diagnostics of Transformers Insulation", IEEE Transactions on Power Delivery, Vol.12, n^o4, pp.1555-1561, October 1997.
- [29] Simulink, "Dynamic System Simulation for Use with Matlab", User's Guide, MathWorks Inc., Natick, MA, 2004.
- [30] Stoenescu E., Popescu M.C., Bulucea C.A., "Assessment of Improved Transformer Thermal Models", Proceedings of the 11th International Conference on Mathematical Methods and Computational Techniques in Electrical Engineering, Published by WSEAS Press, pp.189-195, Vouliagmeni Beach, Greece, September 2009.